Results on Technotest subproject: correlation between material properties, processing and characteristics of Si detectors irradiated by neutrons

E. Verbitskaya, V. Eremin, A. Ivanov, I. Ilyashenko
Ioffe Physico-Technical Institute of Russian Academy of Sciences
St. Petersburg, Russia
Z. Li
Brookhaven National Laboratory, Upton, NY, USA
J. Haarkoonen, E. Tuovinen, P. Luukka
Helsinki Institute of Physics, CERN/PH, Geneva, Switzerland
M. Micuz, V. Cindro, I. Mandic
Iosef Stefan Institute, Ljubljana
Chris Parkes
Glasgow University

5 RD50 Collaboration Workshop
Florence, Oct 13-16, 2004

Technotest

Goal of the project:

Finding correlations and comparison of radiation hardness with respect to:

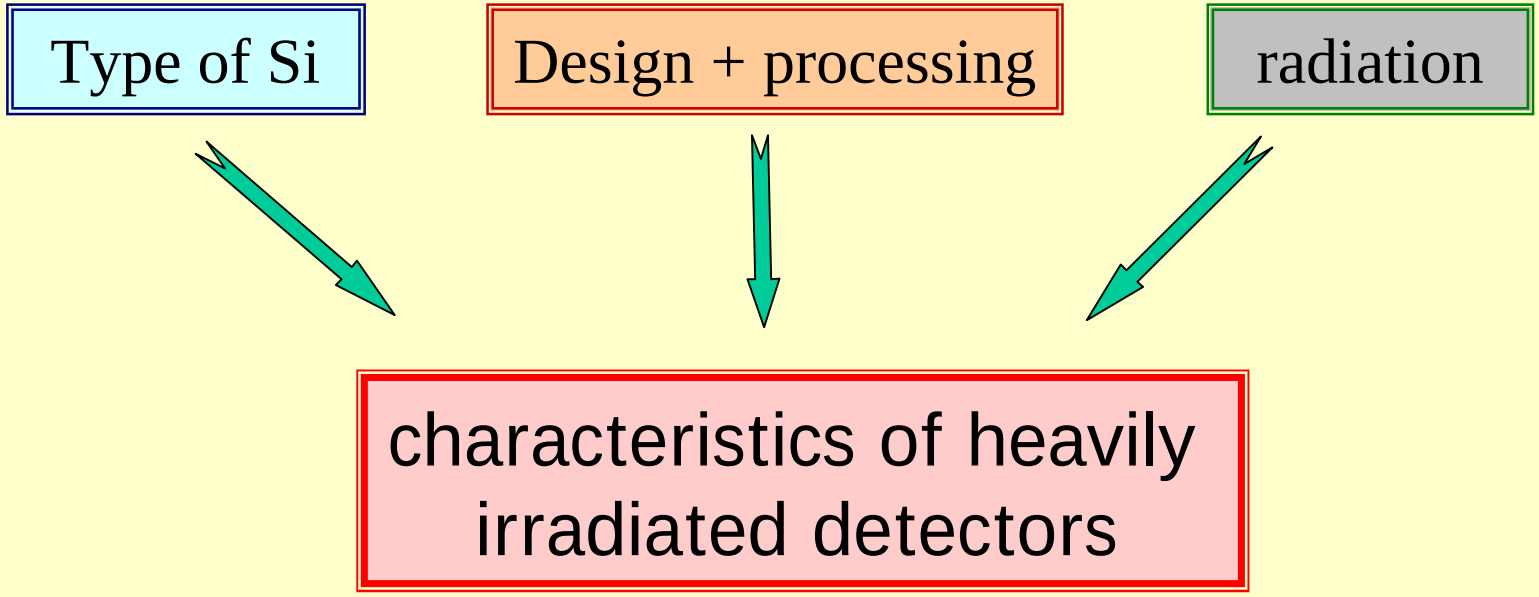

E. Verbitskaya et al., 5 RD50 Workshop, Florence, Oct 13-16, 2004

Technotest

Head: Vladimir Eremin

Participants

Detector processing:

? Ioffe Physico-Technical Institute (PTI)
+ Research Institute of Material Science and Technology (RIMST)
? BNL
? Helsinki Institute of Physics (HIP)

Irradiation:

? CERN (protons 24 GeV)
? Iosef Stefan Institute, Ljubljana (neutrons 1 MeV)

Evaluation

? Ioffe Physico-Technical Institute
? BNL
? HIP
? Iosef Stefan Institute
? Glasgow University
? ITEP, Moscow

Status of the work

Current study:

- **detectors processed at three institutions**
- **Irradiated by 1 MeV neutrons, $F_n = 1 \times 10^{10} - 5 \times 10^{15}$ cm^{-2}**

Types of Si

	BNL	***HIP***	***Ioffe***
n-Si FZ (Wacker)			
p-Si FZ (Wacker)		-	-
n-Si CZ	-		

Resistivity, kΩ·cm
n-Si FZ: 4-6
p-Si FZ: 2-6
n-Si CZ: 1

E. Verbitskaya et al., 5 RD50 Workshop, Florence, Oct 13-16, 2004

Experimental

Detectors irradiated by 1 MeV neutrons, $F_n = 1 \cdot 10^{11}$-$5 \cdot 10^{15}$ cm^{-2}

Fn (cm-2)	n-Si Wacker				n-Si CZ		p-Si Wacker
F1	BNL-n-81	HIP-n-24	PTI-n1-A12	PTI-n2-C11*	HIP-CZ-40	PTI-CZ-A13	BNL-p-83
1.0E+11	BNL-n-82*	HIP-n-43	PTI-n1-B13	PTI-n2-D11	HIP-CZ-51	PTI-CZ-A14	BNL-p-118
F2	BNL-n-111	HIP-n-56	PTI-n1-A11	PTI-n2-A12	HIP-CZ-14	PTI-CZ-C12	BNL-p-78
5.0E+13	BNL-n-131	HIP-n-57	PTI-n1-B11	PTI-n2-B12	HIP-CZ-34	PTI-CZ-D12	BNL-p-95
F3	BNL-n-85	HIP-n-7	PTI-n1-B10	PTI-n2-B13	HIP-CZ-23	PTI-CZ-C11	BNL-p-79
5.0E+14	BNL-n-98	HIP-n-33	PTI-n1-C10	PTI-n2-C13	HIP-CZ-66	PTI-CZ-D11	BNL-p-94
F4	BNL-n-112	HIP-n-13	PTI-n1-A13	PTI-n2-C12	HIP-CZ-7	PTI-CZ-A12	BNL-p-92
1.0E+15	BNL-n-123	HIP-n-23	PTI-n1-A14	PTI-n2-D12	HIP-CZ-45	PTI-CZ-B12	BNL-p-96
F5	BNL-n-84	HIP-n-14	PTI-n1-A10	PTI-n2-A13	HIP-CZ-56	PTI-CZ-A11	BNL-p-97
3.0E+15	BNL-n-122	HIP-n-55	PTI-n1-C11	PTI-n2-A14	HIP-CZ-75	PTI-CZ-B11	BNL-p-106
F6	BNL-n-99	HIP-n-32	PTI-n1-B12	PTI-n2-A11	HIP-CZ-13	PTI-CZ-B13	BNL-p-82
5.0E+15	BNL-n-132	HIP-n-76	PTI-n1-C12	PTI-n2-B11	HIP-CZ-77	PTI-CZ-C13	BNL-p-107

E. Verbitskaya et al., 5 RD50 Workshop, Florence, Oct 13-16, 2004

Experimental

Characterization:

- I-V measurements
- C-DLTS
- TCT using laser pulse generation of free carriers

E. Verbitskaya et al., 5 RD50 Workshop, Florence, Oct 13-16, 2004

I-V characteristics n-Si FZ

$F_n = 1 \cdot 10^{11}\text{-}5 \cdot 10^{15}$ cm^{-2}

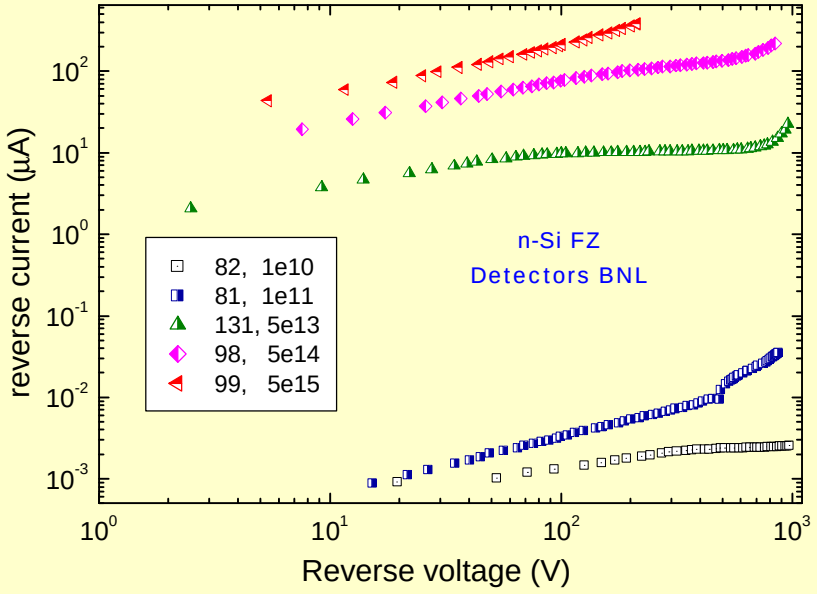

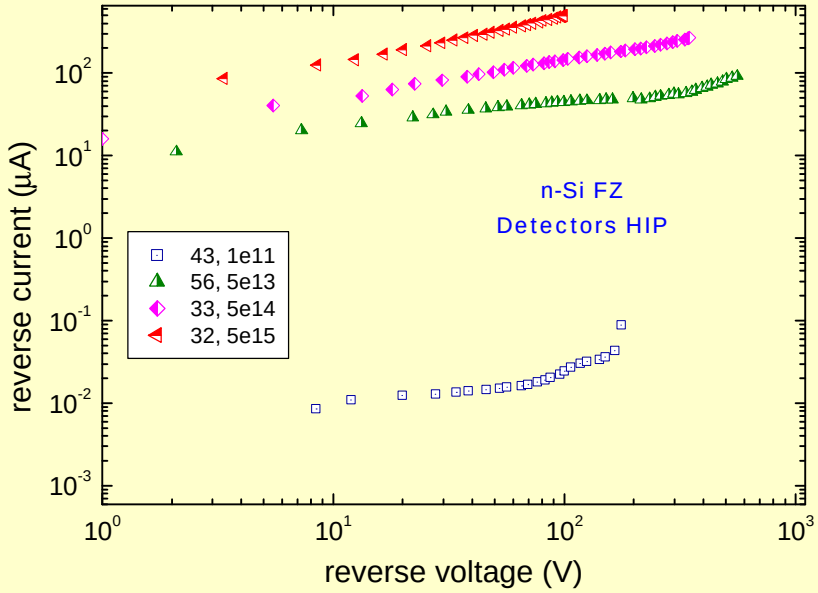

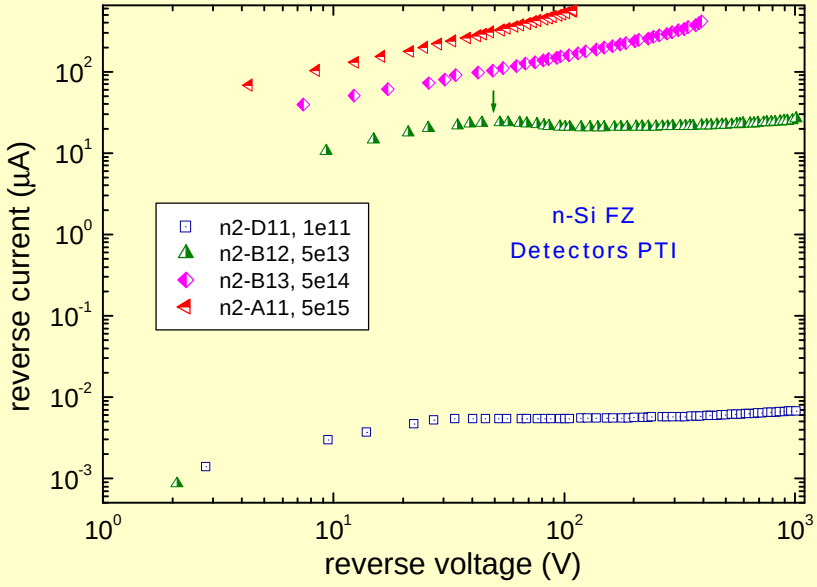

- Saturation for F ≤5 ·10^{13} cm^{-2}
- Current "bump" specific for SCSI for PTI at 5 ·10^{13} cm^{-2}
- Difference can be obviously seen in current density

E. Verbitskaya et al., 5 RD Workshop, Florence, Oct 13-16, 2004

I-V characteristics n-Si CZ

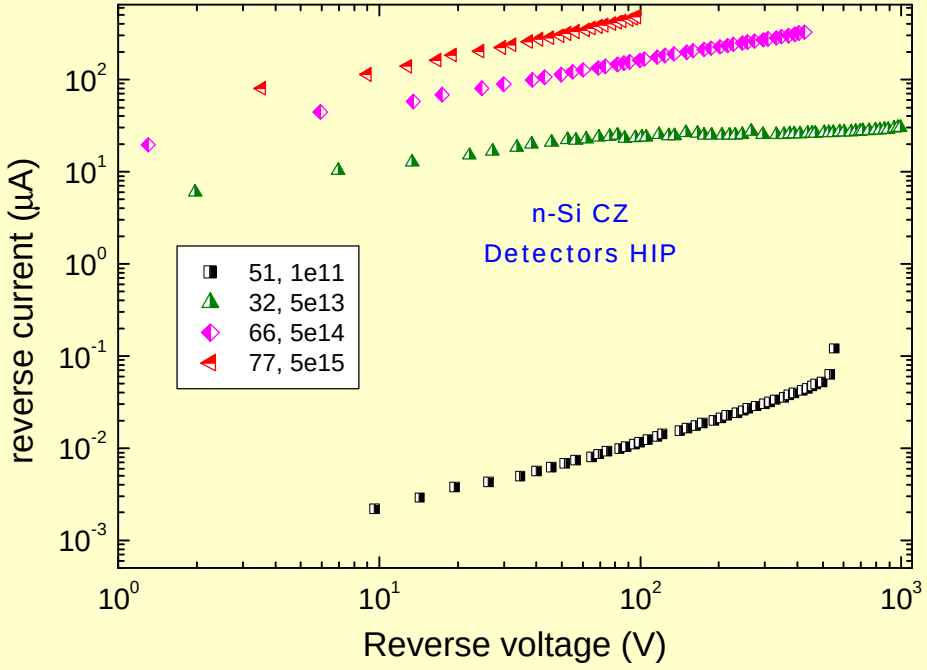

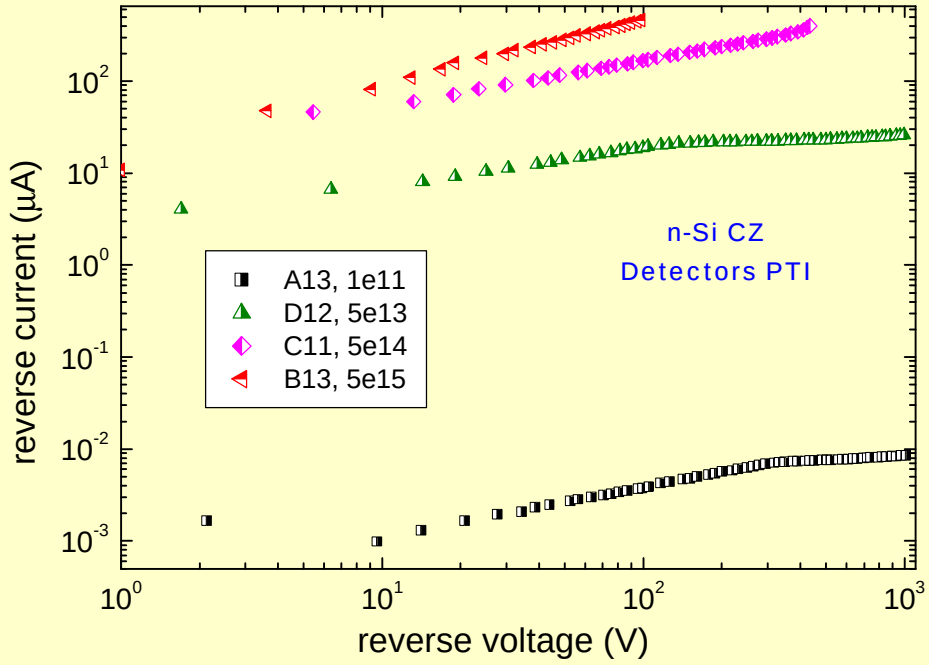

Results on current are similar (except $1 \cdot 10^{11}$ cm^{-2})

F = $5 \cdot 10^{13}$ cm^{-2} – saturation at lower V for HIP

E. Verbitskaya et al., 5 RD50 Workshop, Florence, Oct 13-16, 2004

I-V characteristics: comparison between n-type and p-type FZ Si

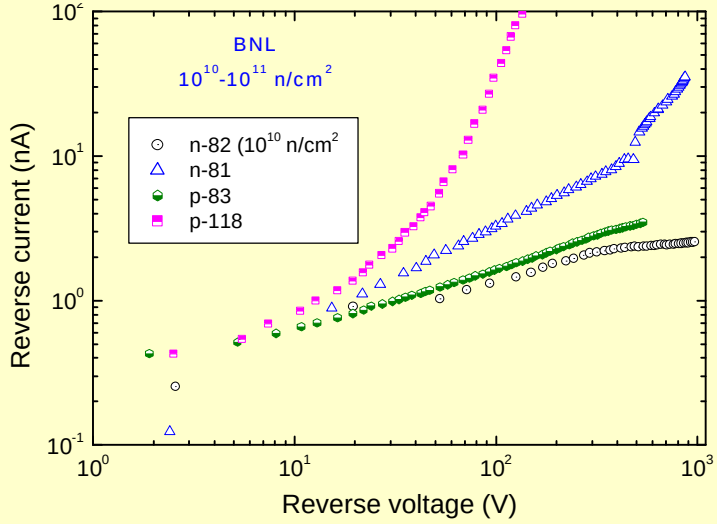

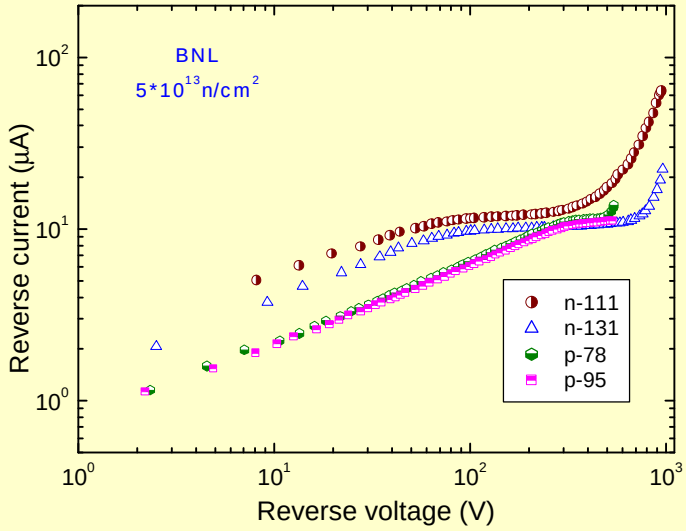

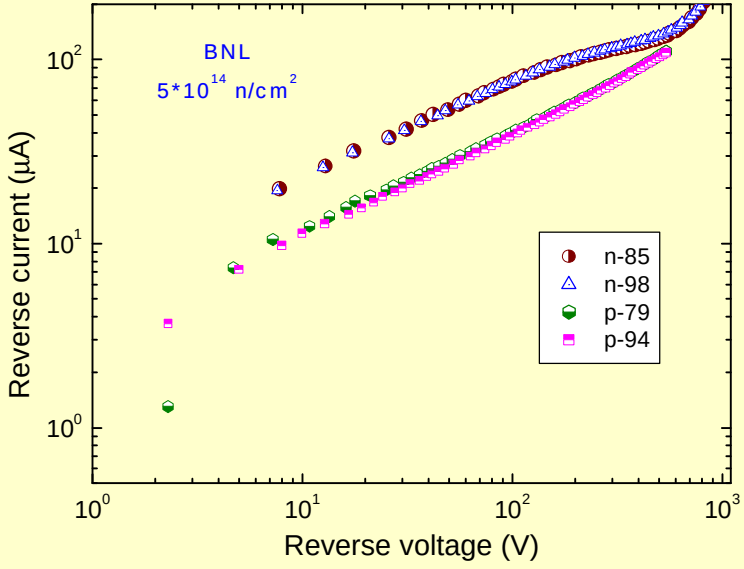

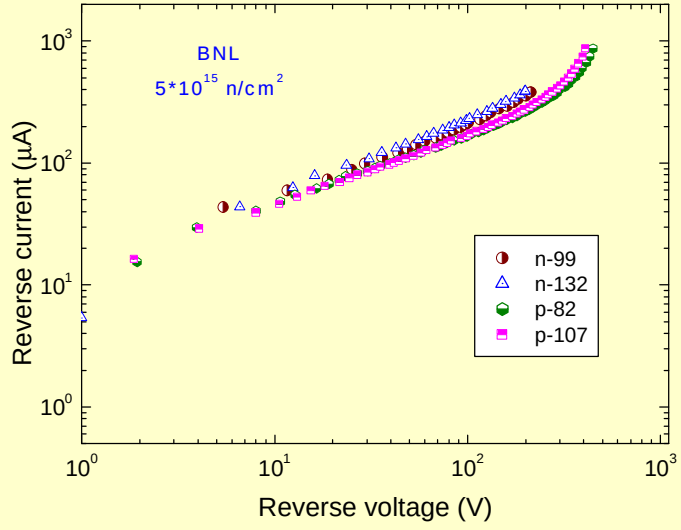

E. Verbitskaya et al., 5 RD50 Workshop, Florence, Oct 13-16, 2004

Current density vs. bias voltage

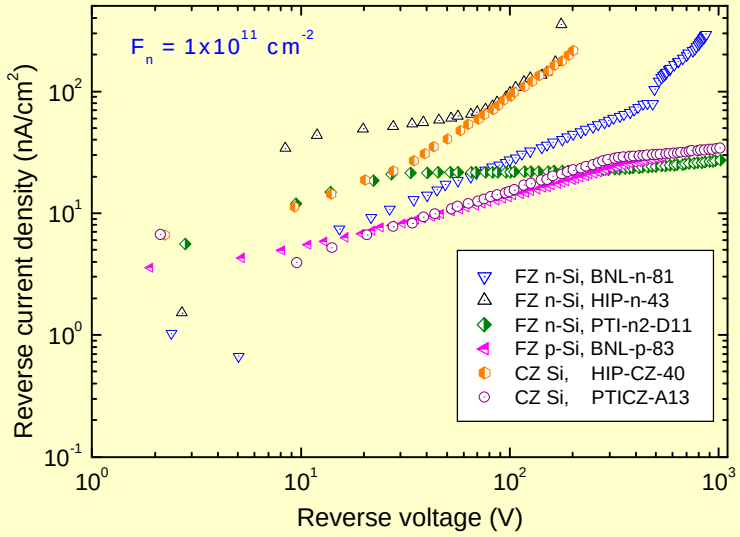

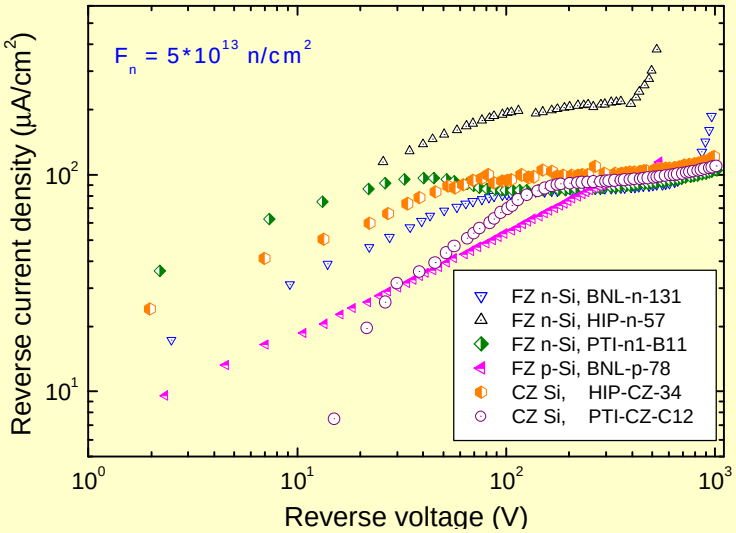

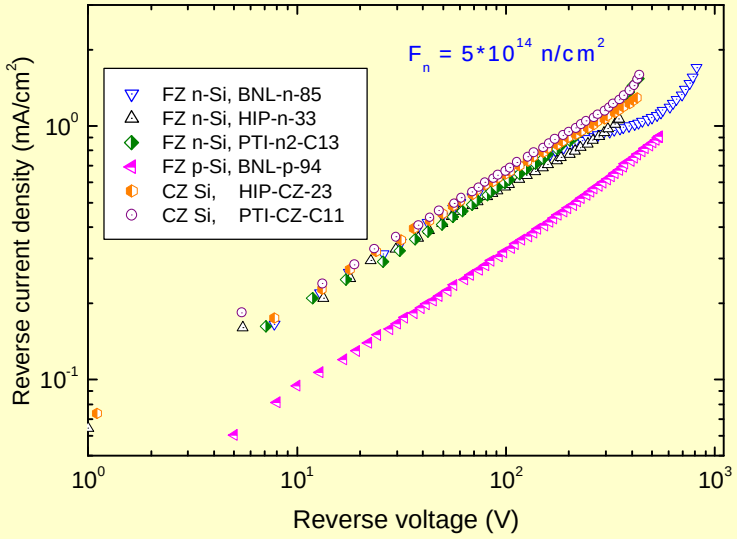

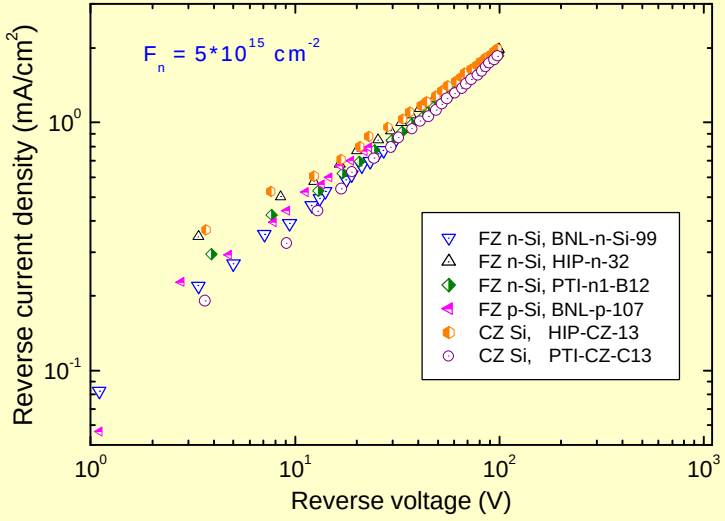

At very high fluence the difference becomes negligible!

E. Verbitskaya et al., 5 RD Workshop, Florence, Oct 13-16, 2004

Defects in FZ Si induced by processing and radiation

1×10^{11} n/cm^2

C-DLTS spectra **no injection** **BNL-n-81: only RD** **with injection**

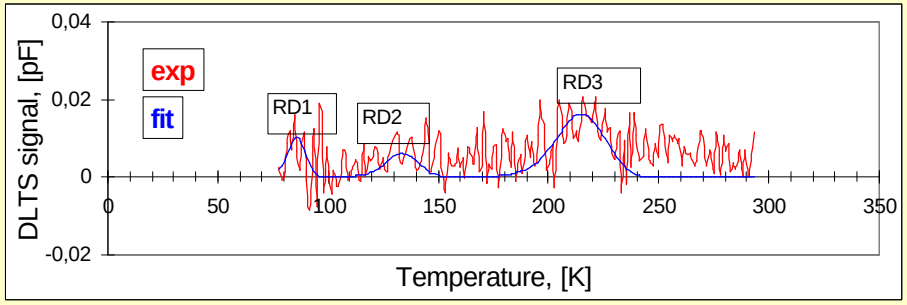

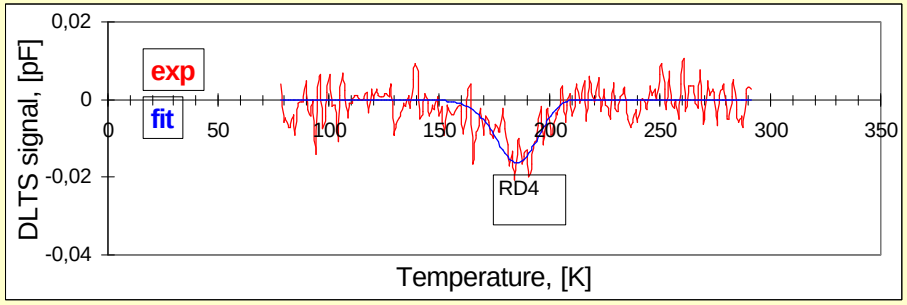

HIP-n-24: TID (E) + RD

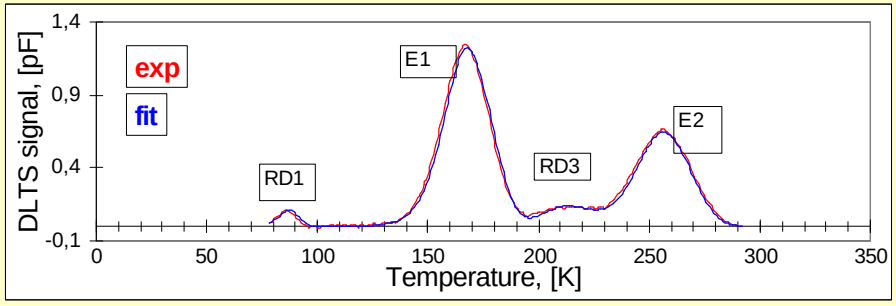

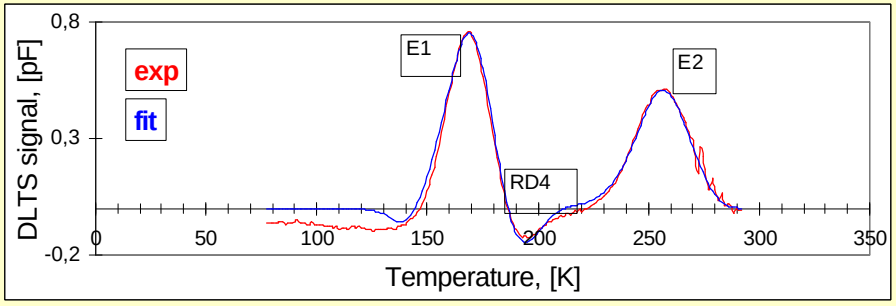

PTI-n1-B13: TID+RD

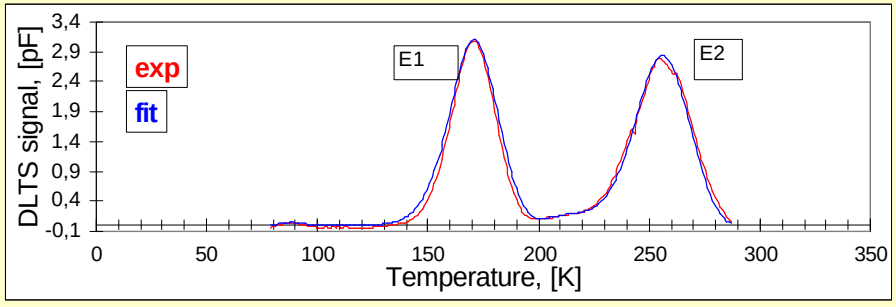

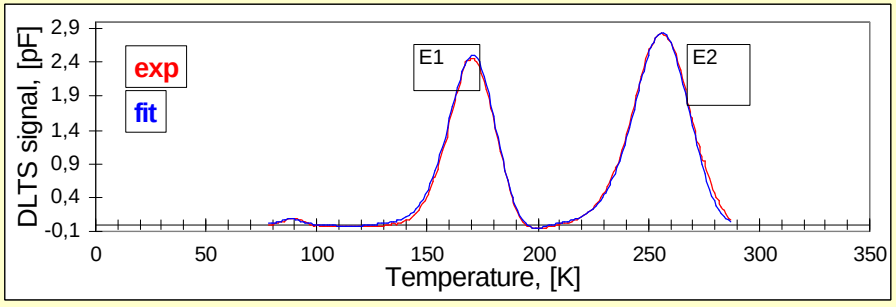

E. Verbitskaya et al., 5 RD50 Workshop, Florence, Oct 13-16, 2004

Comparison of defects in FZ and CZ

FZ, PTI-n1-B13

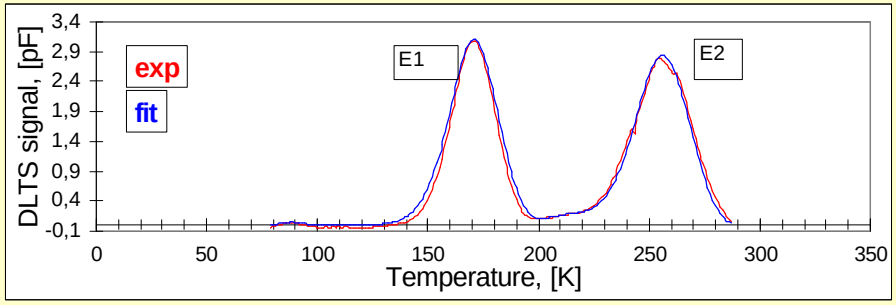

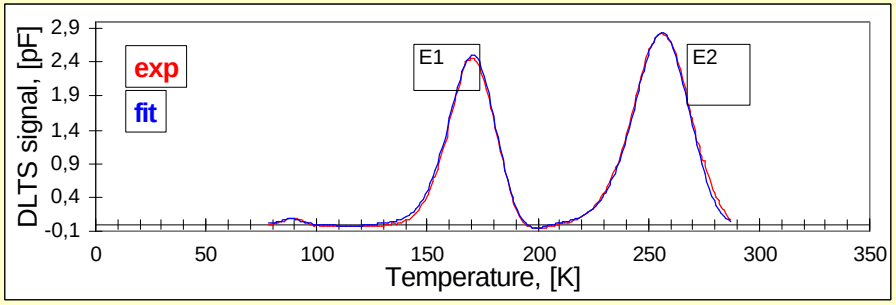

CZ, PTI-Cz-A14

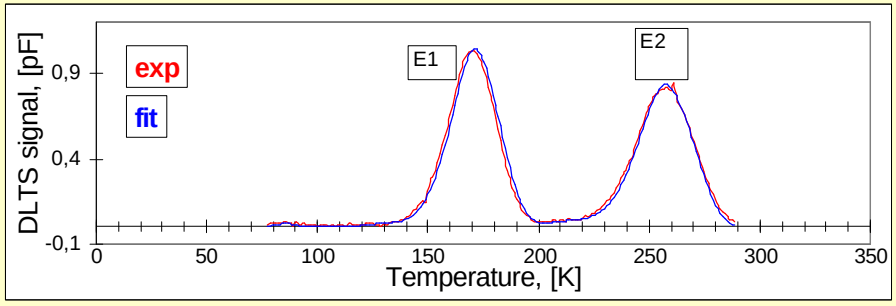

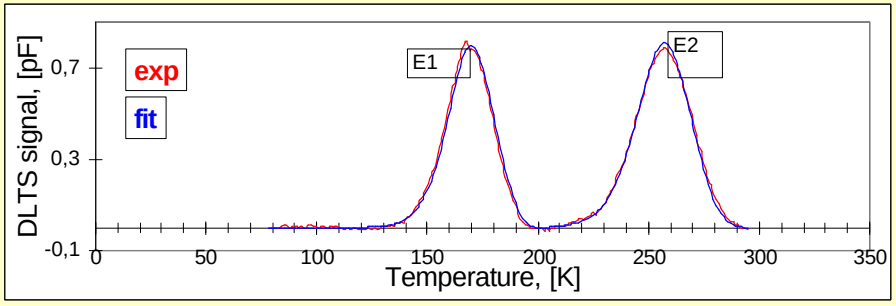

E. Verbitskaya et al., 5 RD50 Workshop, Florence, Oct 13-16, 2004

Table of defects

$F_n = 1 \times 10^{11}$ cm^{-2}

Energy of level (eV)	concentration (cm^{-3})					defect
	n-Si FZ				n-Si CZ	
	BNL-n-82	BNL-n-81	HIP-n-24	PTI-n1-B13	PTI-Cz-A14	
$E_C - 0.181$	$2.5 \cdot 10^9$	$5.0 \cdot 10^9$	$4.6 \cdot 10^9$	$5.2 \cdot 10^9$	$6.8 \cdot 10^9$	**RD1: VO**
$E_C - 0.24$	$3.0 \cdot 10^9$	$3.0 \cdot 10^9$			$6.0 \cdot 10^9$	**RD2: V2(=)**
$E_C - 0.27$			$5.4 \cdot 10^{10}$	$4.0 \cdot 10^{11}$	$4.0 \cdot 10^{11}$	**TID: E1**
$E_C - 0.42$	$7.5 \cdot 10^9$	$8.0 \cdot 10^9$	$6.0 \cdot 10^9$	**2.0×10^{10}**	**1.0×10^{10}**	**RD3: V2(–)+VP**
$E_C - 0.555$			$3.1 \cdot 10^{10}$	$4.6 \cdot 10^{11}$	$3.3 \cdot 10^{11}$	**TID: E2**
$E_V + 0.36$	$9.0 \cdot 10^9$	$8.0 \cdot 10^9$	$1.0 \cdot 10^{10}$	$3.6 \cdot 10^{10}$	$7.6 \cdot 10^9$	**RD4: C_iO_i**

? **TID – Thermally Induced Defects,**
detected in HIP and PTI,
none in BNL, reproducible result

? **RD3: less in CZ than in FZ (PTI)**

E. Verbitskaya et al., 5 RD50 Workshop, Florence, Oct 13-16, 2004

Current pulse response, FZ n-Si, $F_n = 5 \times 10^{13}$ cm^{-2}

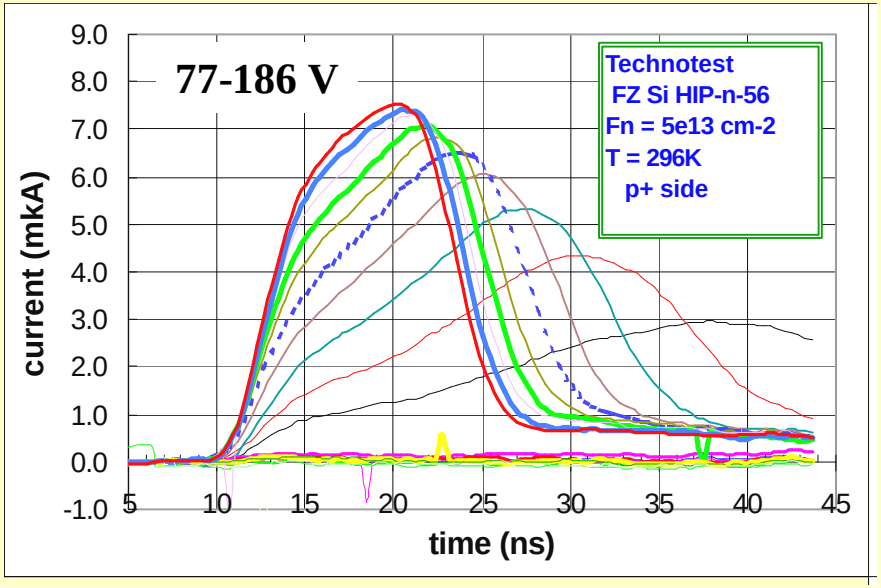

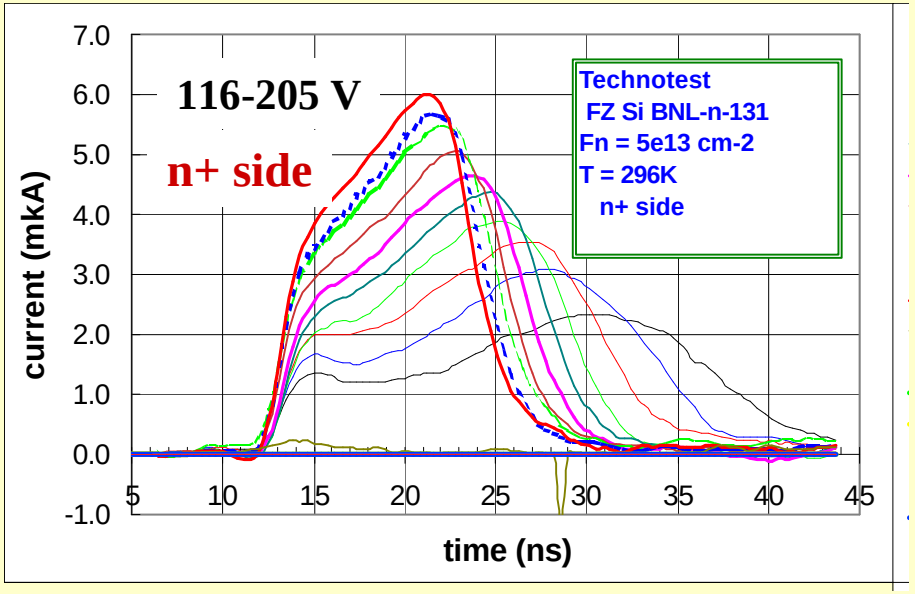

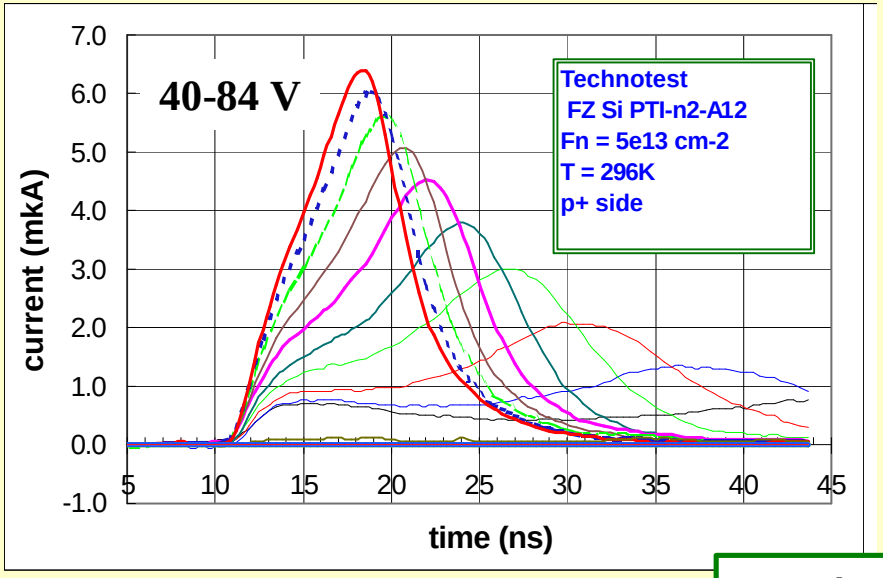

- Slope of pulse top different
- **No SCSI in BNL**
- SCSI in HIP and PTI, V_{fd} different (lower for PTI)

E. Verbitskaya et al., 5 RD50 Workshop, Florence, Oct 13-16, 2004

Current pulse response, CZ n-Si, $F_n = 5 \times 10^{13}$ cm^{-2}

- **No SCSI in HIP and PTI**
- SCSI fluence is higher for PTI (+N_{eff} is larger)

E. Verbitskaya et al., 5 RD50 Workshop, Florence, Oct 13-16, 2004

Current pulse response, FZ n-Si, $F_n = 5 \times 10^{14}$ cm^{-2}

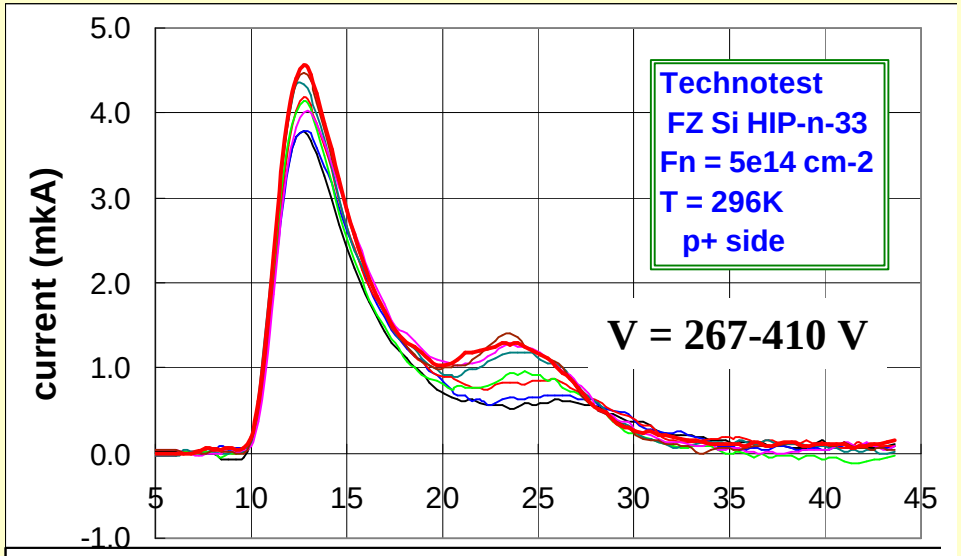

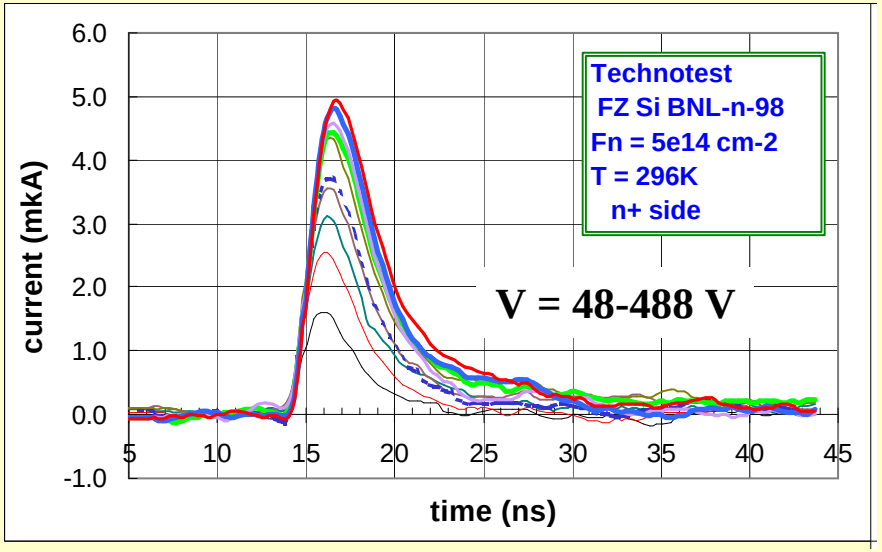

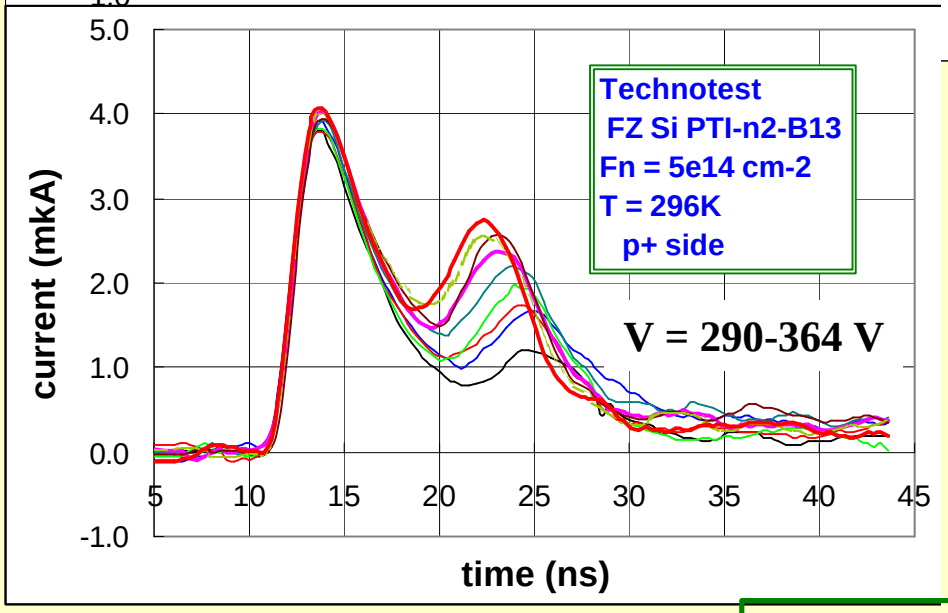

All detectors are beyond SCSI

Difference in DP pulse shape:

HIP: 1st peak dominates at all V

PTI: 2nd peak increases with V

E. Verbitskaya et al., 5 RD50 Workshop, Florence, Oct 13-16, 2004

Current pulse response, CZ n-Si, $F_n = 5 \times 10^{14}$ cm^{-2}

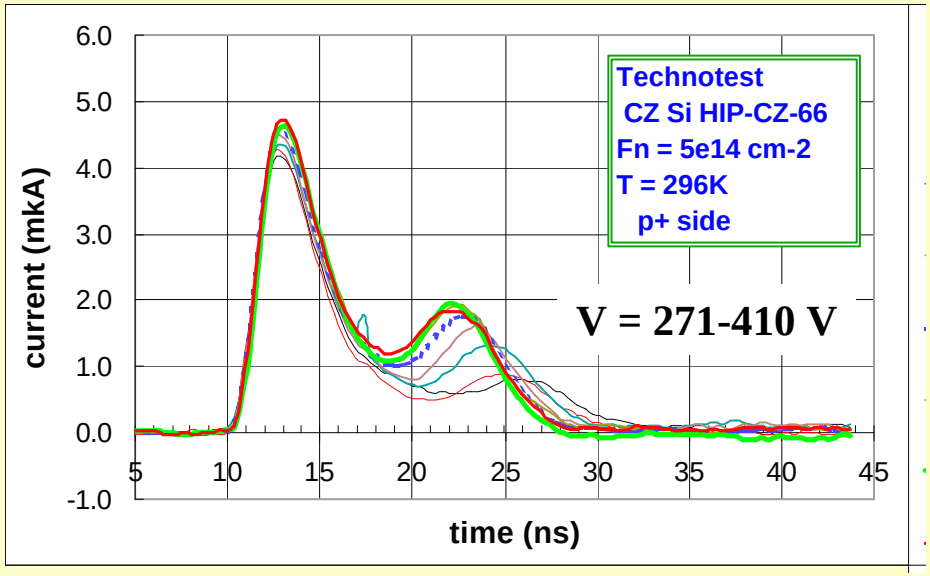

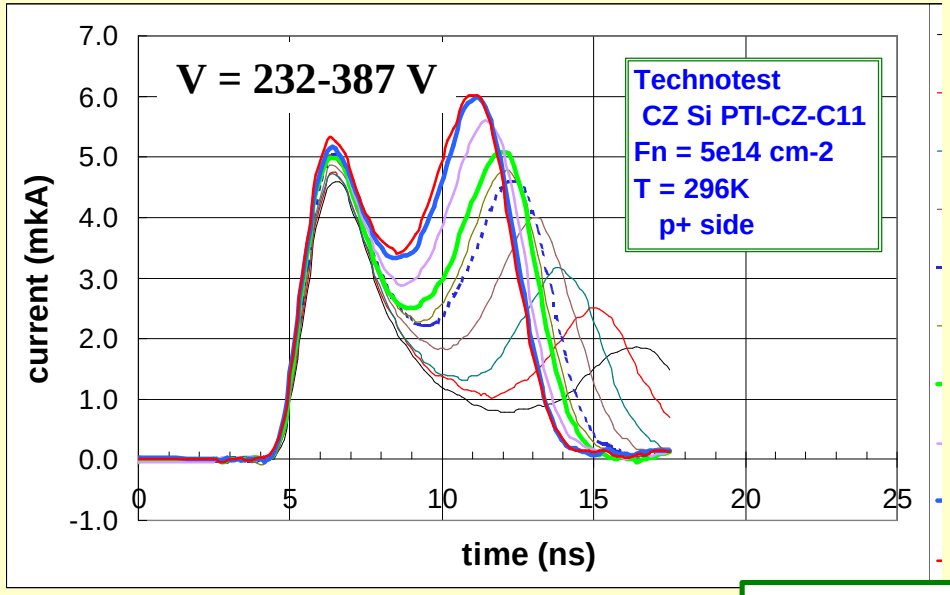

Detectors are beyond SCSI

Difference in DP pulse shape:

- **CZ Si:**

HIP: 1st peak dominates at all V

PTI: 2nd peak increases with V and becomes dominating

V_{fd} is lower in PTI

- **Comparison with FZ Si:**

Increase of the 2nd peak with V is larger in CZ Si

E. Verbitskaya et al., 5 RD50 Workshop, Florence, Oct 13-16, 2004

Simulation of detector response and reconstruction of E(x)

Approach: E. Verbitskaya et al, 5 RESMDD

CZ n-Si, $F_n = 5 \times 10^{14}$ cm^{-2}, V » 350 V

E(x) beyond SCSI

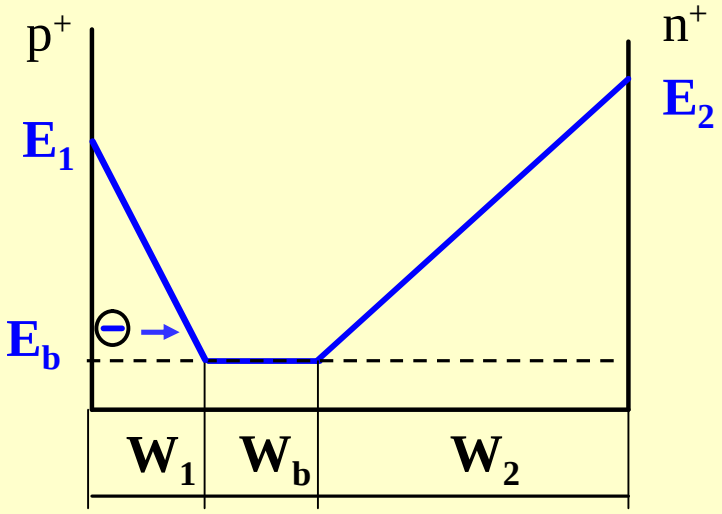

W_1 – major depleted region
W_2 – minor depleted region
W_b – base region with electric field

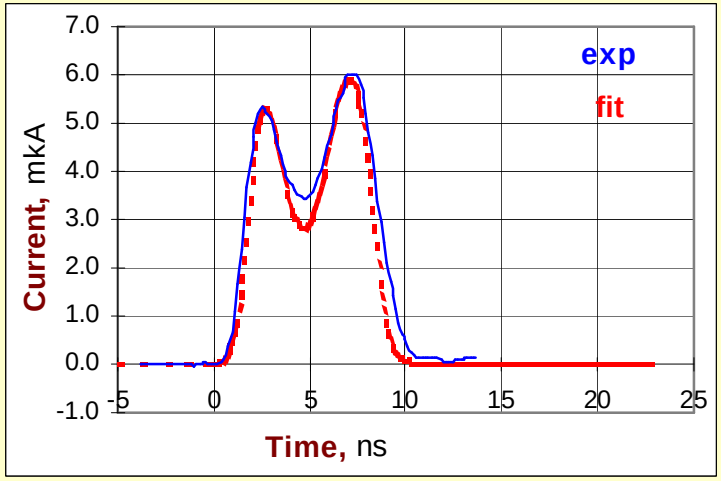

PTI-CZ-C11

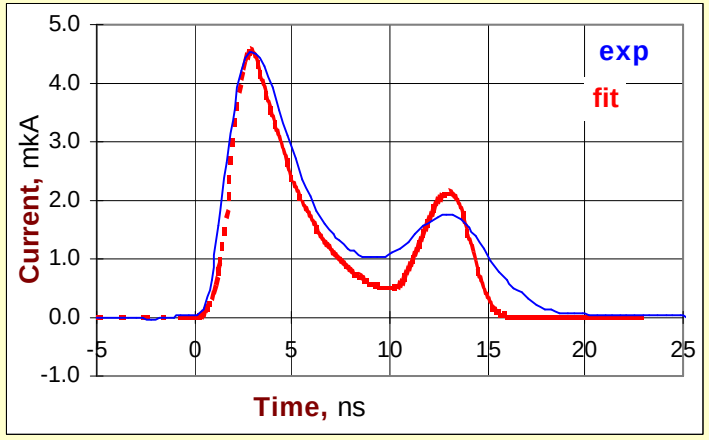

HIP-CZ-66

E. Verbitskaya et al., 5 RD50 Workshop, Florence, Oct 13-16, 2004

Reconstruction of E(x) from detector response

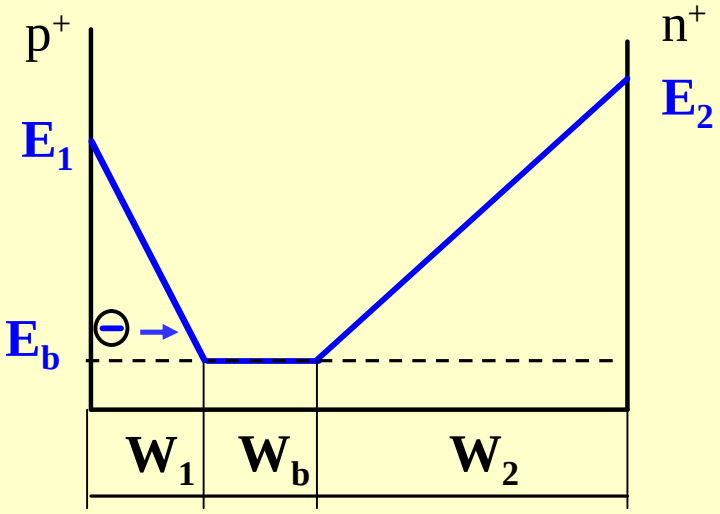

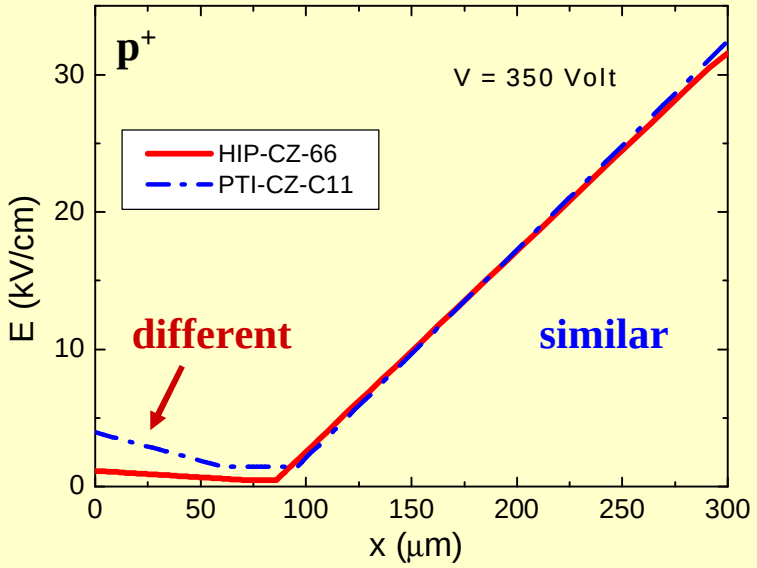

	HIP-CZ-66	PTI-CZ-C11
tau_e (ns)	4	5
Neff1 (cm-3)	1.41E+11	1.09E+12
Neff2 (cm-3)	9.46E+12	9.51E+12
E_b (V/cm)	500	1500

Shape of response and E(x) depend on Si type, and for the same type of Si – on detector processing Þ

Balance of DDs and DAs induced by radiation is sensitive to the type of Si and detector processing

E. Verbitskaya et al., 5 RD50 Workshop, Florence, Oct 13-16, 2004

CCE versus shaping time for p-on-n detectors

$F_n = 5 \times 10^{14}\ cm^{-2}$

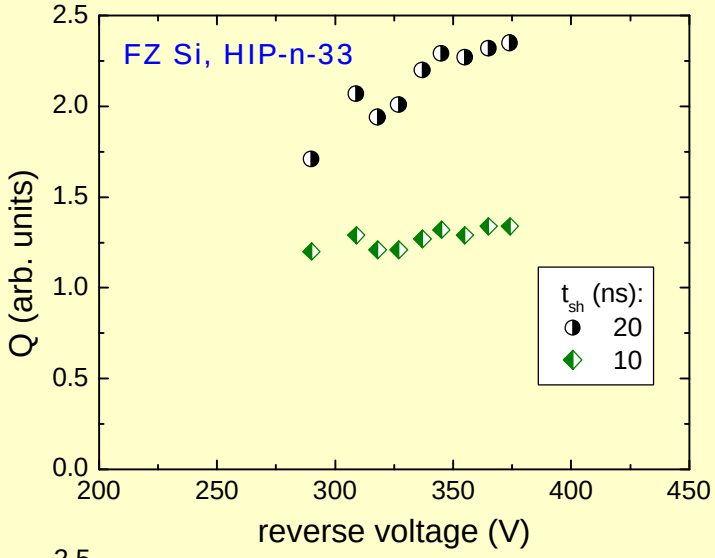

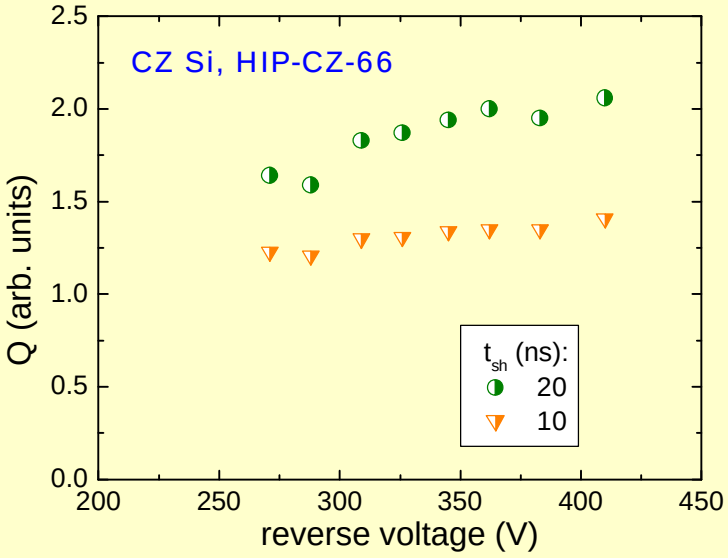

Shaping time 10 ns: CCE increase with voltage is less sensitive to the Si type and processing

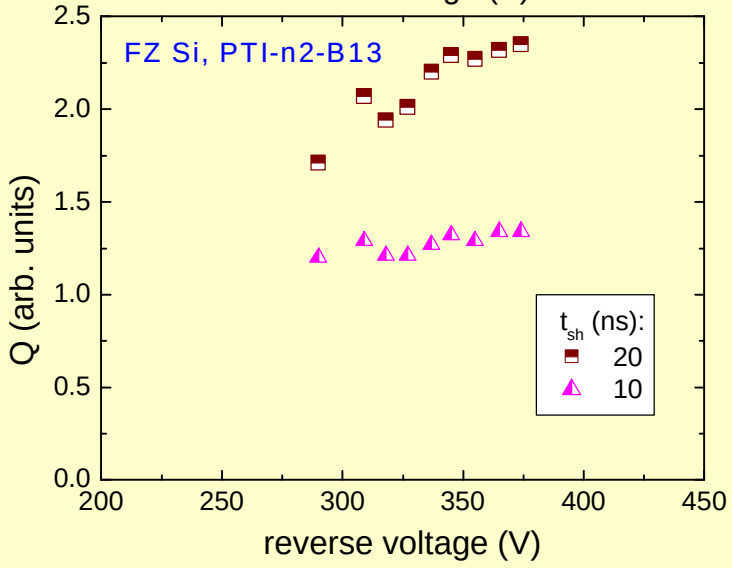

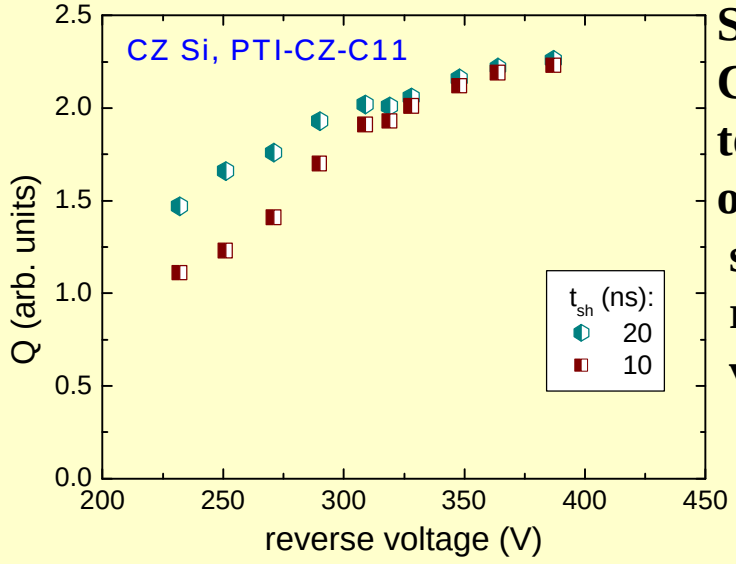

Shaping time 20 ns: CCE correlates to the evolution of specific DP shape of detector response with voltage

E. Verbitskaya et al., 5 RD50 Workshop, Florence, Oct 13-16, 2004

CCE versus shaping time

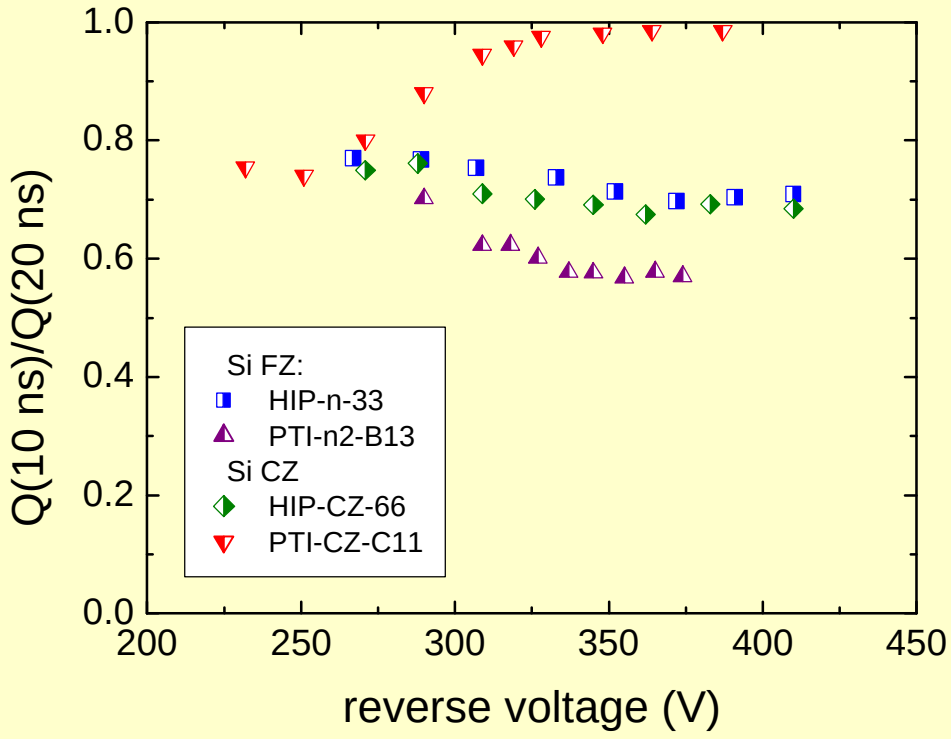

HIP FZ and CZ Si:
1st peak of DP shape dominates, since E in minor depleted region W_1 and W_b is low, therefore CCE is less dependent on shaping time

PTI CZ Si:
2nd peak increases with V since more carriers can reach the major depleted region W_2 adjacent to n^+ contact due to higher E in minor depleted region W_1 near p^+ contact

Estimation corresponds to design of ATLAS strip detectors

E. Verbitskaya et al., 5 RD50 Workshop, Florence, Oct 13-16, 2004

Future study

- Evaluation of detectors irradiated at $F_n \geq 10^{15}$ cm^{-2}
- Evaluation of detectors processed from p-type Si
- Evaluation of proton irradiated detectors
- Study of segmented (strip) detectors

  Strip detectors are already processed in PTI and irradiated by protons

E. Verbitskaya et al., 5 RD50 Workshop, Florence, Oct 13-16, 2004

Conclusions

1. **As-processed detectors:**
   - difference in spectra of thermally induced defects is observed

2. **Irradiated detectors**:
   - FZ Si detectors: SCSI fluence is higher for BNL detectors (as compared to HIP and PTI)
   - CZ Si detectors: SCSI fluence is higher for PTI detectors (as compared to HIP)

3. Double Peak shape response is observed for all detectors irradiated beyond SCSI

4. Treatment of DP response shows:
   - the same E(x) distribution in depleted region extending from n^+ contact
   - higher E in depleted region extending from p^+ contact in PTI detectors

5. Balance of DDs and DAs induced by radiation
   is sensitive to the type of Si and detector processing

Acknowledgement

The study is carried out within the scope of RD50 Collaboration program

and supported in part by:

INTAS project # 03-52-5744,
Department of Energy, USA

Thank you for attention!